Ocean and Coastal Management 255 (2024) 107237

Contents lists available at ScienceDirect

Ocean and Coastal Management

journal homepage: www.elsevier.com/locate/ocecoaman

On the Bruun Rule suitability for modelling shoreline change

Avidesh Seenath [a,*], Jonathan Dale [b]

[a] Environmental Change Institute, School of Geography and the Environment, University of Oxford, United Kingdom
[b] Department of Geography and Environmental Science, University of Reading, United Kingdom

ARTICLE INFO

Keywords:
Bruun rule
Shoreline modelling
Sea-level rise
Sandy coasts
Coastal management

ABSTRACT

Modelling and understanding shoreline response to sea-level rise over decadal to centennial timescales is crucial for managing sandy coasts. Globally, the Bruun Rule is one of the most common shoreline model applied to facilitate this. However, there are several limitations to the Bruun Rule, which can compromise coastal management decisions. Here, we provide a novel assessment of the suitability of the Bruun Rule for application in sandy coasts by applying it to hindcast and project shoreline change in three morphologically different sandy beaches over yearly and decadal timescales. We also compare the Bruun Rule predictions against associated observations, published predictions from a hybrid shoreline model, and historical shoreline changes. Results show that the Bruun Rule fails to accurately hindcast and provide realistic projections of future shoreline change in sandy coasts. We attribute this to the Bruun Rule's assumption of linearity between shoreline retreat and relative sea-level rise and its inability to account for nearshore circulation. We, therefore, recommend limiting the use of the Bruun Rule for informing policy and the management of sandy coasts.

1. Introduction

Recent estimates indicate that 680 million people live in low-lying coastal zones, with this number projected to increase to over one billion by 2050 (Pörtner et al., 2019). In 1990, a global vulnerability assessment estimated that over 200 million people were living below the 1-in-1000-year storm surge level (Hoozemans et al., 1993). These people and assets are at risk of shoreline retreat and inundation from sea-level rise anticipated from climate change, particularly those in small islands (Nicholls and Cazenave, 2010; Nurse et al., 2014; Mycoo and Donovan, 2017; Cutler et al., 2020). As a result, there is an increasing need to predict future meso-timescale (10^1–10^2 years) shoreline change, the primary timescale over which sea-level rise effects are likely to manifest and affect coastal systems (Stive et al., 2002; Van Maanen et al., 2016; Burningham and French, 2017; Hallin et al., 2019; Vousdoukas et al., 2020). Although predictions of meso-timescale shoreline change is becoming of global importance, we need to be aware that shoreline change over this timescale can also be affected by local drivers that operate over smaller micro timescales (<10^1 years), including waves, tidal currents, storm surges, supra-, inter-, and sub-tidal morphology, sedimentology, vegetation, and human influences (Stive et al., 2002; Cooper and Pilkey, 2004; Meyer et al., 2008; Cooper et al., 2018; Almeida et al., 2021; Itzkin et al., 2022).

While there is significant awareness of the influence local drivers have on shoreline change (Ashton and Murray, 2006; Slott et al., 2010; Barkwith et al., 2014), the most common model applied for simulating shoreline change, the Bruun Rule, is a simple linear model that does not account for these factors (Bruun, 1954; Le Cozannet et al., 2014, 2019; Kinsela et al., 2020; Nguyen and Takewaka, 2020). The Bruun Rule assumes the active coastal profile, defined as the area extending from the beach berm (D_b) to closure depth (D_c) – the depth beyond which there is no significant cross-shore sediment transport – maintains a time-averaged equilibrium shape and shifts upward and landward in response to relative sea-level rise (*SLR*) while preserving mass (Fig. 1) (Bruun, 1962, 1983, 1988):

$$R = SLR\left(\frac{L}{D_b + D_c}\right) \quad \text{Eq. 1}$$

where R = shoreline retreat and L = cross-shore distance between D_b and D_c. The wider theoretical assumptions of the Bruun Rule are that: the upper beach erodes due to the landward translation of the active coastal profile; the material eroded from the upper beach is deposited offshore, such that the volume eroded = volume deposited; the rise in the nearshore bottom from deposition is equivalent to *SLR*, maintaining a constant water depth offshore (Bruun, 1962, 1983, 1988). These assumptions have three limitations, as outlined below.

* Corresponding author.
E-mail address: avidesh.seenath@eci.ox.ac.uk (A. Seenath).

https://doi.org/10.1016/j.ocecoaman.2024.107237
Received 3 January 2024; Received in revised form 1 June 2024; Accepted 16 June 2024
Available online 18 June 2024

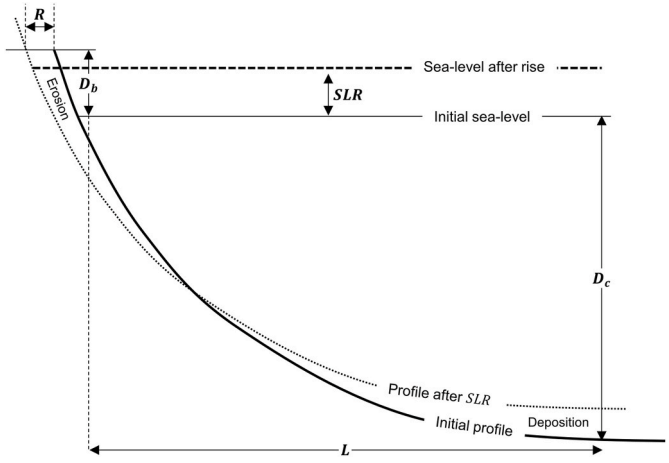

Fig. 1. The Bruun Rule model of shoreline retreat, adapted from Bruun (1962). *SLR* pushes the active coastal profile (D_b to D_c) upward and landward. D_b = beach berm and D_c = closure depth. This translation causes the upper beach to retreat (R), and the eroded material is deposited offshore. The rise in the nearshore bottom from deposition is equivalent to the increase in sea-level, maintaining a constant water depth offshore.

The *first* limitation of the Bruun Rule is an inability to account for nearshore circulation and associated longshore sediment transport, which is often the main driver of shoreline change in sandy coasts, as sediments eroded onshore are assumed to be deposited offshore. Yet, the Bruun Rule is extensively applied to sandy coasts globally, with recent applications in African (Sharaan and Udo, 2020), Asian (Ritphring et al., 2018; Udo and Takeda, 2018; Bagheri et al., 2023), Caribbean (Mueller and Meindl, 2017; Pathak et al., 2021), and European (Thiéblemont et al., 2019; Athanasiou et al., 2020) sandy coasts. While there is considerable awareness of the Bruun Rule's limitations, its continued application in sandy coasts is due to the assumption that it offers a practical method for projecting mesoscale (10^1–10^2 years; 10^1–10^2 km) shoreline change as no simple and viable alternative model exists for such large scale applications (Ritphring et al., 2018; Udo and Takeda, 2018; Thiéblemont et al., 2019; Sharaan and Udo, 2020; Bagheri et al., 2023).

The Bruun Rule's continued application in sandy coastal systems is also linked to the assumption that *SLR* is the main driver of mesoscale shoreline change in these systems, which it explicitly accounts for unlike other shoreline models (Seenath, 2022b). However, a key challenge of applying the Bruun Rule in sandy coasts, which are largely affected by longshore sediment flux, is the considerable uncertainty in associated shoreline change predictions as it only considers cross-shore transport, which may have implications for ensuing coastal management decisions. Given the uncertainty around predictions of future climate change, it is prudent to ensure that we minimise the uncertainties in shoreline change predictions, particularly as these are used to inform decisions for building the adaptive capacity of vulnerable sandy coasts (Seenath et al., 2016; Le Cozannet et al., 2019). Therefore, as Cooper et al. (2020) argue, we need to establish new reliable methods for predicting and understanding shoreline response to natural (e.g., hydrological) and human (e.g., management) forcings instead of continuing to apply flawed modelling approaches.

A second limitation of the Bruun Rule is that it has limited applicability in complex morphologies, defined by shore-perpendicular depth contours, which characterise vulnerable sandy coasts in many small islands. Arguably, these are the locations where shoreline models are most needed as coastal management tools because they: (a) represent the most vulnerable locations to *SLR*; (b) are heavily dependent on coastal resources for livelihoods and economic growth; (c) have limited scope for inland migration of people in response to shifting shorelines (Nurse et al., 2014; Seenath, 2022b; Vousdoukas et al., 2023). This second limitation stems from the Bruun Rule's equilibrium profile assumption that the active coastal profile shifts upward and landward in response to *SLR*. The preservation of the coastal profile shape implicitly implies that the local wave climate is temporally and spatially constant, which further imply that the closure depth is also temporally and spatially constant. These underlying assumptions of the Bruun Rule lead to a gross overgeneralisation of the active coastal profile in complex morphologies where there are significant variations in wave climate and closure depth longshore, which can compromise the credibility of shoreline change predictions (Eversole and Fletcher, 2003; Seenath, 2022b). The idealised morphology assumptions of the Bruun Rule, thus, limits its application to long straight natural sandy shorelines with shore-parallel depth contours (USACE, 2003; McLean, 2013; Pathak et al., 2021). Yet, there is recent evidence of the Bruun Rule's continued application in non-idealised settings, such as the complex tropical sandy coastlines of South America and the Caribbean (e.g., Hippensteel, 2019; Paneque and Finkl, 2020).

The *third* limitation of the Bruun Rule is an inability to predict the longshore evolution of spits and deformations from natural (e.g., oblique waves) and human (e.g., coastal structures) forcings as the active coastal profile is assumed to retreat shore-normal in response to *SLR*. This limitation stems from the idealised morphology assumptions of the Bruun Rule. As per these assumptions, the initial (pre-simulation) and final (post-simulation) active coastal profiles are in equilibrium; a constant coastal profile shape is maintained over the time period considered; the total quantity of sediment in the cross-section is conserved (Bruun, 1962, 1983, 1988). However, these assumptions are not appropriate for application in sandy coasts (a) with coastal structures, which often modify the shape of the coastal profile and shoreline by intercepting longshore sediment transport and affecting nearshore circulation; (b) where spits form in response to wind-wave action (McLean, 2013). Yet, in recent years, the Bruun Rule has also been applied in sandy coasts in many small islands, Japan, Egypt, and Malaysia that are modified by coastal structures and geomorphological agents (e.g., wind-wave action), which it does not account for (e.g., Ritphring et al., 2018; Sharaan and Udo, 2020; Pathak et al., 2021; Bagheri et al., 2023).

Despite these limitations, the Bruun Rule is the only model that explicitly links shoreline change to *SLR* (Sharaan and Udo, 2020), which is often regarded as the main driver of mesoscale coastal change (Nicholls et al., 1996; Stive et al., 2002; Hallin et al., 2019; Vousdoukas et al., 2020). It, therefore, forms the basis of several mesoscale shoreline models (see, e.g., Álvarez-Cuesta et al., 2023), including the Shoreface Translation Model (Cowell et al., 1992), SimCLIM (Warrick, 2009) and CoSMoS-COAST (Robinet et al., 2018). Given its ability to facilitate mesoscale applications and account for *SLR*, more recent studies that have applied a form of the Bruun Rule for modelling shoreline change have adopted probabilistic approaches (e.g., Ranasinghe et al., 2012; Thiéblemont et al., 2021; Dastgheib et al., 2022; Masselink et al., 2022). Probabilistic modelling accounts for the effects of intrinsic uncertainty in models, which, in the case of the Bruun Rule, stems from the data used to specify its parameters (Thiéblemont et al., 2021; Dastgheib et al., 2022). This type of modelling also enables an investigation into the potential outcomes (in this case, shoreline response) that may occur due to natural variability in climatic or stochastic forcing conditions (Stripling et al., 2017). Probabilistic modelling, therefore, makes coastal managers aware of the uncertainties in shoreline change predictions and the potential implications that may arise from ensuing coastal management decisions (Stripling et al., 2017). Although probabilistic approaches consider the intrinsic uncertainty of models, using theoretically and physically flawed models to predict shoreline change will still inevitably present a challenge for coastal management decisions (Le Cozannet et al., 2019; Cooper et al., 2020; Ranasinghe, 2020).

Despite considerable theoretical criticisms of the Bruun Rule (see Cooper and Pilkey, 2004), its suitability for modelling mesoscale

shoreline change is not yet invalidated primarily because of a global lack of decadal-scale coastal data to assess and verify its assumptions (Le Cozannet et al., 2019; Tinh et al., 2021). Cooper et al. (2020) argue that shorelines *will* and *must* retreat as sea levels rise, which is the basic premise of the Bruun Rule. Therefore, the Bruun Rule's linear representation of the relationship between *SLR* and shoreline change may, *in theory*, be adequate for simulating and understanding mesoscale shoreline change. However, until there is *empirical evidence* that either validates or invalidates the Bruun Rule, the optimal complexity for modelling mesoscale shoreline change will remain largely uncertain.

Therefore, in this study, we empirically assess the Bruun Rule for modelling micro and meso-timescale shoreline change in sandy coasts, which are affected by coastal processes and local factors that it does not explicitly consider (e.g., longshore sediment flux, complex morphology, and coastal structures). Our aim here is to assess the suitability of applying the Bruun Rule in such environments, where there appears to be a recurring misapplication of the Rule. We consider the micro-timescale because if a model cannot predict realistic shoreline change over this timescale, the errors introduced will accumulate and generate unreliable predictions over longer timescales (Seenath, 2022b). Specifically, we.

(a) apply the Bruun Rule to hindcast micro-timescale shoreline change in three morphologically different sandy beaches and compare the results against corresponding observations and predictions from Seenath (2022b) hybrid shoreline models.
(b) apply the Bruun Rule to hindcast meso-timescale shoreline change in a sandy barrier island and compare the results against corresponding observations and published predictions from Seenath (2022a) hybrid shoreline models.
(c) apply the Bruun Rule and a hybrid shoreline model to project meso-timescale shoreline change in a sandy barrier island and a fringing reef coastal system in response to a future *SLR* scenario. We compare the results against historical meso-timescale shoreline change observed under past *SLR* in both locations.

Our approach enables a unique assessment of the Bruun Rule's suitability for modelling shoreline change in sandy coasts, providing critical insights into the kinds of sandy coastal environments that it is most applicable for. Such an approach also enables us to identify which model structures produce the most reliable shoreline change predictions in sandy coasts, and gauge the relative impact of *SLR* and other geomorphological agents on shoreline change longshore in these systems. The findings will have implications for refining the application of shoreline models to better inform the management of sandy coasts.

2. Methods

2.1. Test sites

To address our aim, we require test sites that represent simple and complex sandy beach morphologies; have open-access high-resolution coastal data (topo-bathymetry, tide, wind, and waves) to enable our modelling campaign; have historical micro and meso-timescale shoreline change observations and verified predictions to benchmark our Bruun Rule results against. Considering these requirements and the hybrid shoreline modelling studies we build upon, we focus on three test sites previously investigated by Seenath (2022b), specifically, sandy beaches in New York, Puerto Rico, and Southern California.

The New York site has a mean tidal range of 1.43 m (microtidal) and spans 12.5 km along the Atlantic coast of Long Beach Barrier Island (Fig. 2). A hold-the-line approach involving 43 groynes and beach feeding is used to stabilise the shoreline, which is concave in the east and west, and mostly straight elsewhere except for deformations around groynes (Fig. 2b). We define the shoreline here and elsewhere as the Mean High Water (MHW) line. The site is characterised by shore-parallel depth contours (simple morphology) and an average coastal profile that gently slopes, decreasing monotonically seaward (Fig. 2c; d).

The Puerto Rico site is also microtidal with a mean tidal range of 0.34 m and spans 5 km along the Atlantic coast of San Juan (Fig. 3). Hold-the-line approaches (breakwaters, seawalls and groynes) are used to stabilise the shoreline, which is also naturally protected by fringing reefs (Fig. 3b). The reefs here mean that the site has a complex morphology, with shore-parallel and shore-perpendicular depth

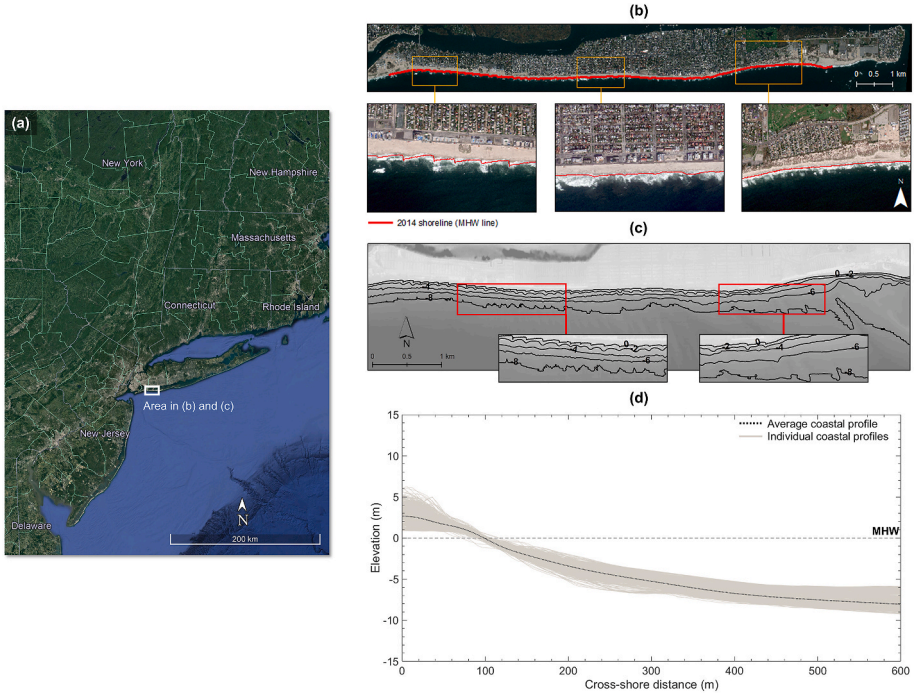

Fig. 2. Test site in New York. (a) Location. (b) Overview of main site features. (c) Nearshore planform morphology. (d) Coastal profile envelope. *Credits*: Google Earth (a) and LAND INFO Worldwide Mapping (b). Modified from Seenath (2022b).

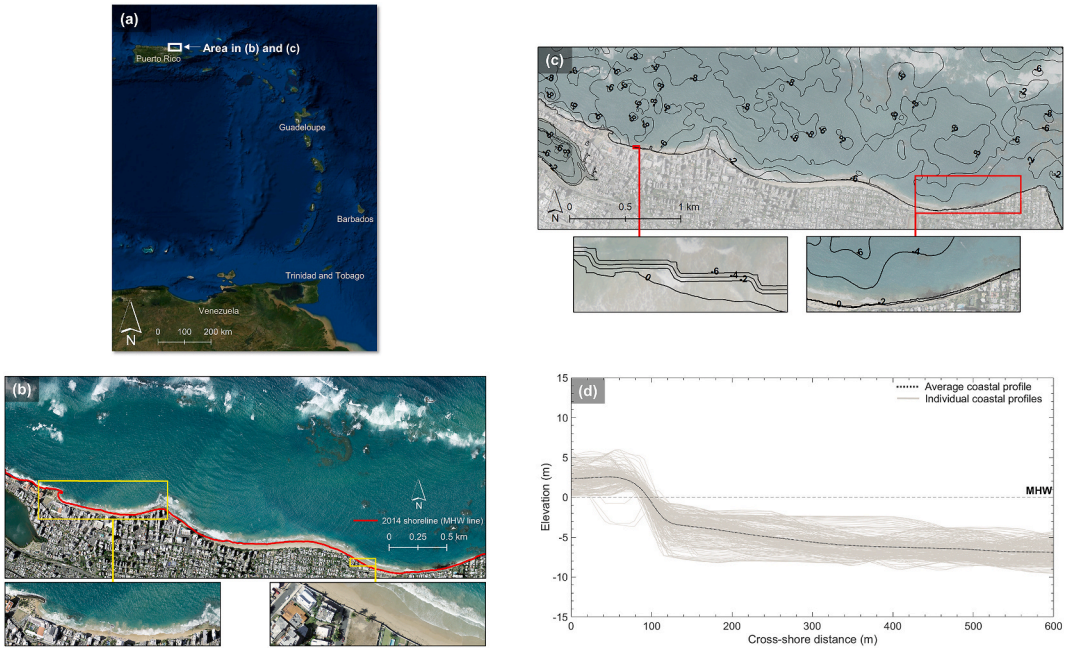

Fig. 3. Test site in Puerto Rico. (a) Location. (b) Overview of main site features. (c) Nearshore planform morphology. (d) Coastal profile envelope. *Credits*: DigitalGlobe (a) and USGS (b). Modified from Seenath (2022b).

contours (Fig. 3c). Hence, there is significant cross-shore variability in the nearshore bed despite the active coastal profile showing a steep upper and gentler lower beach (Fig. 3d).

The Southern California site has a mean tidal range of 1.14 m (microtidal) and spans 11 km along Santa Monica's coastline, California (Fig. 4). Hold-the-line approaches (eight groynes; two jetties) are used to stabilise the shoreline (Fig. 4b), with temporary sand berms built annually for protection against winter storms. The site has a simple morphology, defined by a relatively straight shoreline, except for deformations around groynes, and shore-parallel depth contours (Fig. 4b). Compared to the above sites, this site has a steep average coastal profile that decreases monotonically cross-shore (Fig. 4 c; d).

By focusing on these sites, our study makes a novel assessment of the Bruun Rule's suitability for modelling shoreline change as each site has a distinct morphology influenced by various geomorphological agents (e.g., coastal defences, longshore littoral drift, reefs), some of which the Rule does not account for. Such an assessment allows us to evaluate the extent of the Bruun Rule's suitability in sandy coasts that both conform

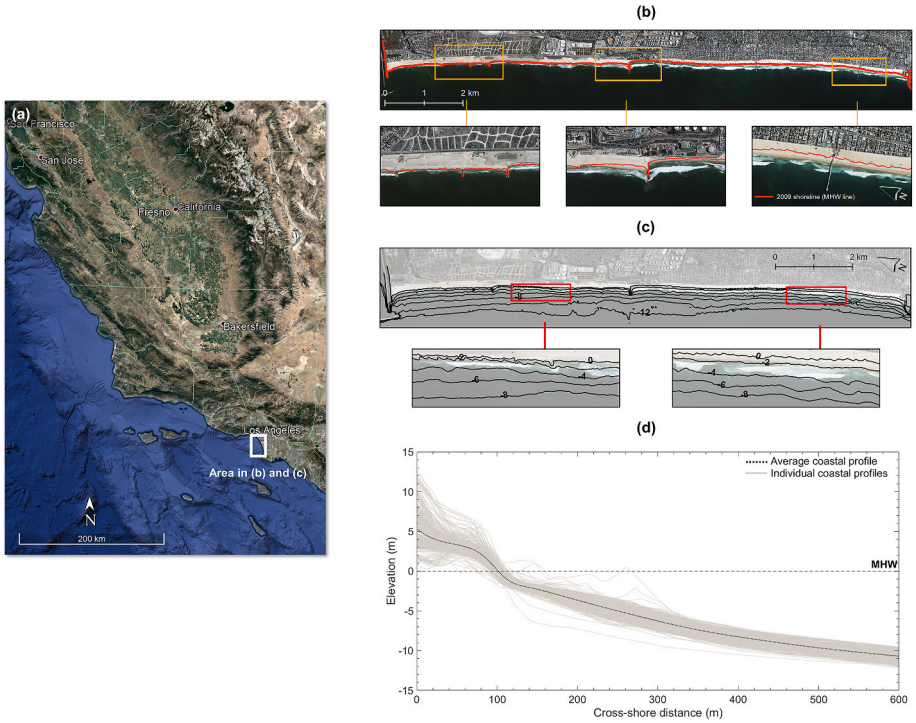

Fig. 4. Test site in Southern California. (a) Location. (b) Overview of main site features. (c) Nearshore planform morphology. (d) Coastal profile envelope. *Credits*: DigitalGlobe (a) and LAND INFO Worldwide Mapping (b). Modified from Seenath (2022b).

and do not conform to its morphology assumptions; assess the relative impact of *SLR* (which drives the Rule) and other geomorphological agents on the evolution of sandy shorelines. Hereafter, we use the following abbreviations: NY = New York test site, PR = Puerto Rico test site, and SC = Southern California test site.

2.2. Model selection, description, and application

2.2.1. Bruun Rule

The original Bruun Rule assumes shoreline retreat is equal to relative sea-level change divided by the upper shoreface slope (Eq. (1)) (Bruun, 1962). This rule relates shoreline retreat (R) to *SLR* by the ratio of the active coastal profile horizontal (L) and vertical dimensions – berm height (D_b) and closure depth (D_c). It assumes that sandy coasts have homogenous sediment properties and simple shoreline geometries (Bruun, 1983). Modified versions of the Rule also assume linearity between *SLR* and shoreline retreat but include additional parameters on heterogeneous coastal material, coastal profiles, and cliff elevation, specific to cliffed coasts and/or atoll islands (Malcolm and Janet, 1997; Cowell and Kench, 2001; Young et al., 2014). Sandy coasts differ from these in sediment sorting, profile shape, and planform evolution (Pontee et al., 2004; Karunarathna et al., 2016). The simple morphology of NY and SC investigated herein conforms to the idealised assumptions of the original Bruun Rule. The complex morphology of PR does not conform to the simple shoreline geometry assumptions of the original and modified versions of the Bruun Rule. However, the assumptions of the original Bruun Rule better characterise the sediment properties at PR. We, therefore, focus on the original Bruun Rule.

We apply the Bruun Rule to cross-shore transects every 5 m longshore to estimate shoreline change in NY and SC. All transects run through the D_b and D_c contours (Fig. 5a). 2449 and 1941 transects are generated in NY and SC, respectively. L (cross-shore distance between D_b and D_c) varies in each transect whereas D_b and D_c are constant. The *SLR* value used to formulate the Bruun Rule in these sites are derived from their *SLR* rate: 0.004 m yr^{-1} in NY (NOAA, 2017d) and 0.002 m yr^{-1} in SC (NOAA, 2017e).

We follow the same principles above to apply the Bruun Rule at PR, except we vary D_c and L in each transect based on reef substrate distribution (Fig. 5b). At this site, 702 transects are used. In reef transects, D_c = depth nearest the shoreline where reef substrate first appears in line with the closure depth definition established for reef environments (Eversole and Fletcher, 2003). In non-reef transects, D_c = most seaward depth contour that follows the shoreline shape, following Kaergaard and Fredsoe (2013). The *SLR* value used to apply the Rule at PR is derived from the site's *SLR* rate: 0.002 m yr^{-1} (NOAA, 2017c).

2.2.2. MIKE21

We consider Seenath (2022b)'s review of shoreline models and select MIKE21, a hybrid model, for comparison against the Bruun Rule. MIKE21 applies a two-dimensional coupled wave, flow, and sediment transport model to calculate littoral drift gradients in response to natural and human forcings over simple and complex morphologies. It uses these gradients to update the shoreface morphology based on a one-line equation by uniformly distributing the gradients over the active coastal profile (D_b to D_c):

$$\frac{\Delta N}{\Delta t} = \frac{vol}{dA_z} \qquad \text{Eq. 2}$$

where ΔN = horizontal distance over which the shoreline moves perpendicular to its orientation, and dA_z = vertical area of the active coastal profile over which *vol* is uniformly distributed. Sediment gain (loss) over the profile shifts the profile seaward (landward). As the shoreline morphology update is constrained by the one-line equation, MIKE21 can facilitate mesoscale simulations. This computational structure currently offers the best approach for simulating mesoscale shoreline change in simple and complex morphologies (Seenath, 2022b), hence is most suitable for handling the contrasting morphologies of our test sites. Seenath (2022b) established an optimal MIKE21 parameterisation and computational mesh for each site (Table 1; Fig. 6), which we have, therefore, applied in this paper. Please see DHI (2017) for details of MIKE21.

2.2.3. On comparing the Bruun Rule with MIKE21

We recognise that comparing the Bruun Rule with MIKE21 is not without limitations, given the differences in their complexity and capabilities. However, the approach that MIKE21 adopts for updating the shoreline morphology is computationally similar to the Bruun Rule, which tends to be overlooked. For instance, both assume the active coastal profile move shore-normal in response to a change in sediment balance. The *primary* difference between both is that the profile movement in MIKE21 is in response to littoral drift driven by nearshore circulation whereas, in the Bruun Rule, it is in response to the total amount

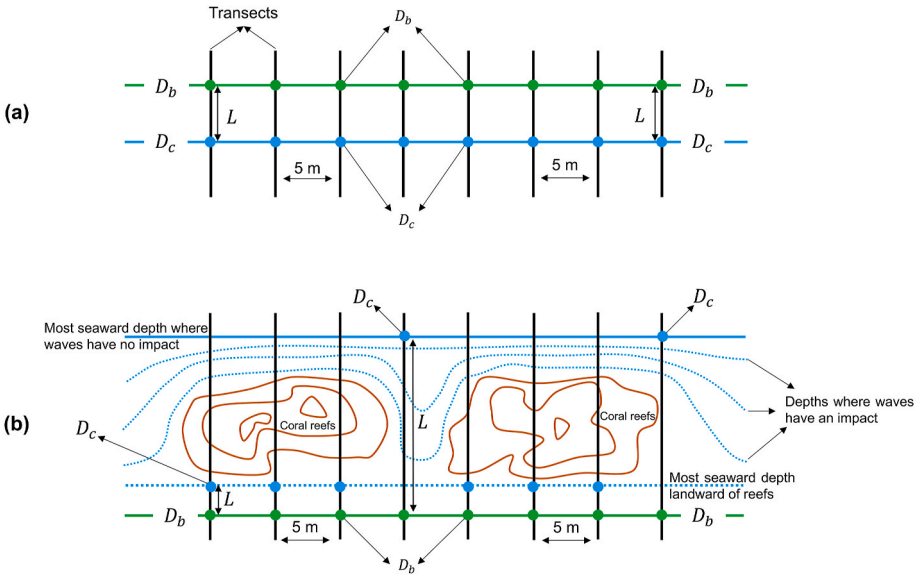

Fig. 5. General formulation of the Bruun Rule in NY and SC (a), and PR (b). D_c and L are the same in all transects in (a) but vary in each transect according to reef substrate distribution in (b). In all cases, we formulate the Bruun Rule in cross-shore transects every 5 m longshore using the same D_b in each transect.

Table 1
Calibrated MIKE21 model established for each site (Seenath, 2022b). Site-specific specifications are indicated by NY = New York test site, PR = Puerto Rico test site, and SC = Southern California test site.

Input	Specifications
General	
Simulation period (micro-timescale hindcast)	NY: 01.01.2014–01.02.2016 PR: 01.10.2014–31.03.2016 SC: 01.01.2009–02.08.2011
Simulation period (meso-timescale hindcast)	NY: 01.01.1966–01.02.2016
Simulation period (meso-timescale project)	NY: 01.01.2014–01.01.2064 PR: 10.10.2014–10.10.2064
Nearshore spatial discretisation[a]	45 m (NY and PR); 30 m (SC)
Offshore spatial discretisation	70 m
Time step interval (output frequency)	86 400 s (daily)
MIKE21 HD	
Coriolis forcing	Varying in domain
Courant-Friedrich-Lévy (CFL) number	0.8
Density	Barotropic
Manning's *n* reciprocal[a]	NY and PR: 29 $m^{1/3}/s$ SC: 33 $m^{1/3}/s$ (SC)
Maximum time step	30 s
Minimum time step	1.21 s
Overtopping discharge[b]	0 $m^3/s/m$
Smagorinsky coefficient (eddy viscosity)	0.28
Wave radiation stresses	Internally transfers from MIKE21 SW
Weir coefficient[a,3]	1.21 $m^{1/2}/s$ (NY); 0.55 $m^{1/2}/s$ (PR); 0.99 $m^{1/2}/s$ (SC)
Tidal forcing	Tide data forced at sea boundary in the domain.
Wind forcing	Wind speed and direction data forced over the domain.
Wind friction (varies based on wind speed)	0.001255 to 0.002425
MIKE21 ST	
Critical Shields parameter	0.05
Grading coefficient[a]	1.1
Grain diameter[a]	0.2 mm (NY and SC); 0.25 mm (PR)
Flow/wave forcing	Internally transfers from MIKE21 SW
Maximum bed level change	10 m/day
Porosity[a]	0.3 (NY and PR); 0.5 (SC)
Relative sand density	2.65
Time step factor	1
MIKE21 SW	
Current conditions (speed and direction)	Internally transfers from MIKE21 HD
Maximum number of iterations	500
Nikuradse roughness	0.04 m
Reflection coefficient (structures)	0.5 (cross-shore structures in each test site) 1 (longshore structures in PR)
Spectral discretisation	360° rose
Water level conditions	Internally transfers from MIKE21 HD
Wave forcing	Wave climate data forced at sea boundary in the domain.
MIKE21 SM	
Berm height	1.14 m (NY); 1.5 m (PR); 2 m (SC)
Closure depth (micro-timescale hindcast)	5.8 m (NY); 3.5–7 m (PR); 5 m (SC)
Closure depth (meso-timescale hindcast)	4.2 m (NY)
Closure depth (meso-timescale project)	5.8 m (NY); 3.5–7 m (PR)
Maximum number of iterations	500
Sediment transport gradients	Internally transfers from MIKE21 ST

[1,3] Used for cross-shore structures (e.g., groynes) in each test site.
[a] Calibrated input.
[b] Used for longshore structures (e.g., seawalls and breakwaters) in the Puerto Rico test site.

of *SLR*. Therefore, while MIKE21 simulates the complex physics of sediment transport, its shoreline morphology update is underpinned by a simple equation (Eq. 2) similar to the Bruun Rule. Uncoupling the sediment transport module from MIKE21 leaves behind a simple one-line equation (Eq. 2), which is based on pre-established rules that conform to the equilibrium beach profile theory and ignores the complexity of the physics underpinning the evolution of coastal profiles, like the Bruun Rule. The littoral drift gradients calculated from the complex sediment transport simulations are solely an input for the one-line equation in MIKE21. Similarly, *SLR*, which is derived from long-term tidal records (representative of local sea-level variations), is an input to the Bruun Rule. Hence, comparing both models allows us to test (a) whether *SLR* is the main driver of meso-timescale shoreline change as assumed in related studies; (b) a behavioural modelling approach, based on the equilibrium beach profile theory (Bruun Rule and one-line models), for updating the shoreline morphology is sufficient for simulating micro and meso-timescale shoreline change.

2.3. Data and study periods

We use the Digital Elevation Models (DEMs) and, tide, wind and wave data in Table 2 to.

(a) hindcast micro-timescale shoreline change in NY (2014–2016), PR (2014–2016), and SC (2009–2011) using the Bruun Rule. We compare the results with corresponding observations and Seenath (2022b)'s MIKE21 predictions.
(b) hindcast meso-timescale shoreline change in NY (1966–2016) using the Bruun Rule. We compare the results with corresponding observations and Seenath (2022a)'s MIKE21 predictions.
(c) project meso-timescale shoreline change (2014–2064) in response to future *SLR* in NY and PR using the Bruun Rule and MIKE21. Here, we aim to evaluate whether the Bruun Rule can provide *theoretically realistic* projections of future shoreline change.

For each site, we obtain an initial and observed DEM, both vertically referenced to MHW (m) and horizontally referenced to WGS 84 (m). The initial DEM provides the observed topo-bathymetry at the start of the simulation. We, therefore, use the initial DEM to: (a) derive D_b, D_C, and L to formulate the Bruun Rule and parameterise MIKE21; (b) interpolate the computational mesh for MIKE21 sediment transport simulations. The observed DEM represents the topo-bathymetry observed at the end of the simulation. We consider the MHW line in each DEM as the shoreline. We use the initial shoreline to map changes in shoreline position, and the observed shoreline to quantify shoreline prediction accuracy.

The tide, wind and wave data provide the boundary conditions in MIKE21 (Table 2). The tide data also underpins the established *SLR* rates for each site (NOAA, 2017d; NOAA, 2017e; NOAA, 2017c), which we use to formulate the Bruun Rule.

We use a 0.5 m resolution GeoEye-1 image of NY, a 0.1 m resolution orthophoto of PR, and a 1 m resolution KOMPSAT-2 image of SC to obtain locational data on site-specific coastal structures. In each site, we use the DEMs obtained to define the elevation characteristics of associated coastal structures.

2.4. Model simulations

2.4.1. Micro-timescale hindcasts

We first assess the Bruun Rule's ability to reliably hindcast micro-timescale shoreline change in each site against corresponding observations and predictions from Seenath (2022b) calibrated MIKE21 models. Here, we formulate the Bruun Rule equation in cross-shore transects every 5 m longshore to hindcast shoreline change from 2014 to 2016 in NY and PR, and 2009–2011 in SC using the following specifications.

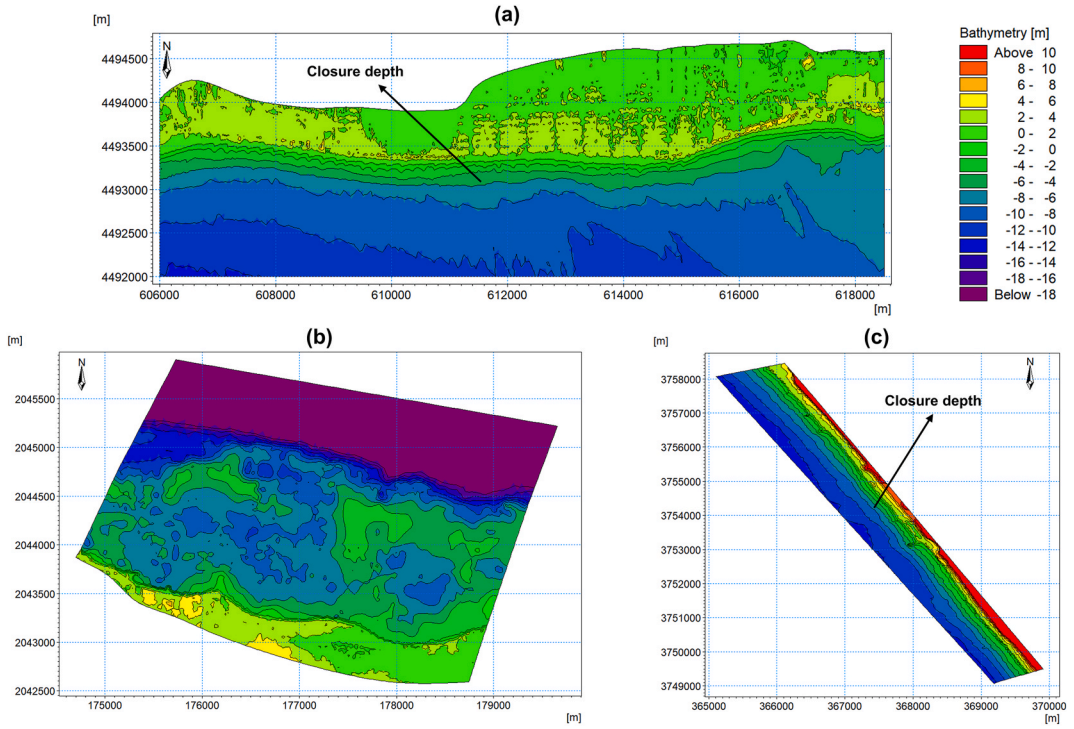

Fig. 6. Computational mesh optimised for MIKE21 application in NY (a), PR (b) and SC (c) (Seenath, 2022b). Each mesh is interpolated with the initial DEM obtained for micro-timescale applications (Table 2).

Table 2
Data used for micro and meso-timescale shoreline simulations in each site.

Data	Time period (dd.mm.yyyy)	Application	Horizontal datum	Vertical datum	Units	Resolution	Source
Initial bathymetry	NY: 01.01.2014	Micro hindcast; meso project	WGS84	MHW	m	3 m	NCEI (2017a)
	NY: 01.01.1966	Meso hindcast				10 m	USGS (2017)
	PR: 01.10.2014	Micro hindcast; meso project				3 m	NCEI (2019)
	SC: 01.01.2009	Micro hindcast				10 m	NCEI (2017b)
Observed bathymetry	NY: 01.02.2016	Micro hindcast; meso hindcast				3 m	NOAA (2017b)
	PR: 31.03.2016	Micro hindcast				3 m	NOAA (2019)
	SC: 02.08.2011	Micro hindcast				1 m	NOAA (2017a)
Tide	NY: 01.01.2014–01.02.2016	Micro hindcast	N/A			6 min	
	NY: 01.01.1966–01.02.2016	Meso applications				60 min	
	PR: 01.10.2014–31.03.2016	Micro hindcast				6 min	NOAA (2017d)
	PR: 01.01.1969–31.12.2018	Meso project				60 min	NOAA (2017c)
	SC: 01.01.2009–02.08.2011	Micro hindcast				6 min	NOAA (2017e)
Wind speed		All applications		N/A	m/s	6 min	
Wind direction	NY: 01.01.2014–01.02.2016				deg.		
Wave height	PR: 01.10.2014–31.03.2016				m	NY; PR: 60 min	NDBC (2017a)
Wave direction	SC: 01.01.2009–02.08.2011				deg.	SC: 30 min	NDBC (2017c)
Wave period					s		NDBC (2017b)

- NY: D_b = 1.14 m above MHW, D_c = 5.8 m below MHW, L varies in each transect, ranging from 184.17 to 447.48 m, and SLR = 0.008 m (NOAA, 2017d).
- PR: D_b = 1.5 m above MHW, D_c varies in each transect based on reef substrate distribution, ranging from 3.49 to 7.97 m below MHW (Fig. 7), L ranges from 61.23 to 836.81 m, and SLR = 0.004 m (NOAA, 2017c).
- SC: D_b = 2 m above MHW, D_c = 5 m below MHW, L ranges from 114.41 to 251.3 m, and SLR = 0.006 m (NOAA, 2017e).

The Bruun Rule has four parameters only: D_b, D_c, L, and SLR. Here and elsewhere, we ensure that the specification of these parameters is the same as those specified in MIKE21 (Table 1).

2.4.2. Meso-timescale hindcast

We next assess the Bruun Rule's ability to reliably hindcast meso-timescale shoreline change (1966–2016) in NY by formulating its equation in cross-shore transects every 5 m longshore, and comparing the results with corresponding observations and predictions from Seenath (2022a) 1966-2016 MIKE21 model for the site (Table 1). The Bruun Rule formulations here are based on the following inputs.

- D_b = 1.14 m above MHW
- D_c = 4.2 m below MHW
- SLR = 0.2 m (NOAA, 2017d)
- L ranges from 292.74 to 491.42 m.

2.4.3. Meso-timescale projections

We conclude our assessment of the Bruun Rule by applying it to project meso-timescale shoreline change from 2014 to 2064 under a 0.28 m SLR in NY and PR by formulating its equation in cross-shore transects every 5 m longshore based on the following specifications:

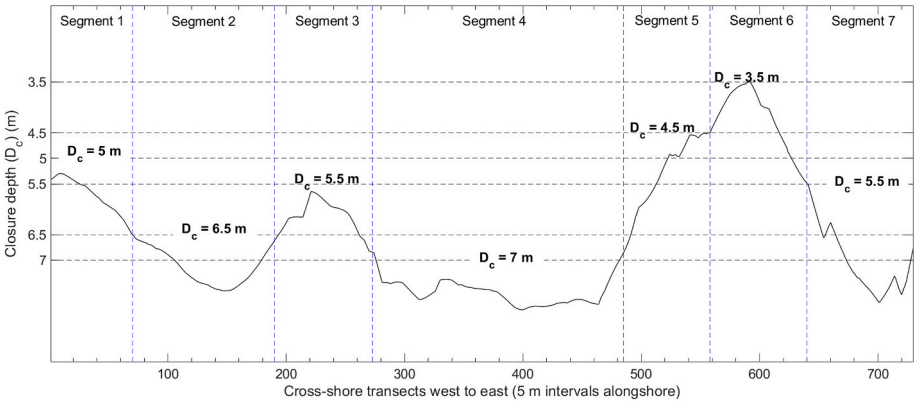

Fig. 7. Closure depths observed (black line) in PR. MIKE21 is not designed to handle longshore variations in the closure depth. We, therefore, divide PR into coastal segments, with each segment having a different closure depth that generalises the underlying morphology of the area, following Seenath (2023).

- NY: $D_b = 1.14$ m above MHW, $D_c = 5.8$ m below MHW, and L varies in each transect, ranging from 184.17 to 447.48 m.
- PR: $D_b = 1.5$ m above MHW, D_c ranges from 3.49 to 7.97 m below MHW based on the spatial distribution of reef substrate, and L ranges from 61.23 to 836.81 m.

We then apply Seenath (2022b)'s calibrated MIKE21 model for NY and PR (Table 1) over the same period, and compare the results from both models with historical observations of meso-timescale shoreline change under similar *SLR* conditions.

2.5. Model accuracy assessment

In each site, we use the cross-shore transects generated, excluding those in locations with coastal structures, to quantify shoreline change observations and predictions. We use the results to calculate the Brier Skill Score (*BSS*) to quantify the accuracy of shoreline predictions:

$$BSS = 1 - \frac{\sum (Sh_{obs} - Sh_{pred})^2}{\sum (Sh_{obs} - Sh_{init})^2} \quad \text{Eq. 3}$$

where Sh_{init} = shoreline position observed at the start of the simulation in each transect, Sh_{pred} = shoreline position predicted at the end of the simulation in each transect, and Sh_{obs} = shoreline position observed at the end of the simulation (baseline) in each transect. The *BSS* is a non-dimensional measure of the accuracy of a prediction relative to a baseline, recommended for verifying coastal morphology models (Sutherland et al., 2004). *BSS* ranges from -∞ to 1, indicating how far a model prediction deviates from the baseline. Here, we treat Sh_{obs} as the baseline for *BSS* calculations. A *BSS* = 1 indicates perfect agreement between Sh_{obs} and Sh_{pred}, 0 indicates that Sh_{pred} is closer to Sh_{init}, and a negative *BSS* indicates that Sh_{pred} is further away from Sh_{obs}. Sutherland et al. (2004) classified a *BSS* of 1–0.5 as excellent, 0.5–0.2 good, 0.2–0.1 reasonable, 0.1–0 poor, and ≤0 bad. We apply the same classification in this paper.

We exclude transects in locations with coastal structures from the *BSS* calculations because both models assume the active coastal profile moves from a change in sediment balance, ignoring the underlying bed features (e.g., elevation, slope, and coastal structures) over which the profile translates. As a result, a coastal structure within a migrating profile will also move with the profile, giving an erroneous estimate of shoreline change and enabling a disingenuous assessment of the accuracy of both models. Less than 5% of transects generated in each site is in areas with coastal structures. Excluding these, the total number of transects used to quantify model accuracy is 2330 in NY, 695 in PR, and 1894 in SC.

3. Results and discussion

The Bruun Rule predicts negligible micro-timescale shoreline change longshore in each site, with magnitudes close to 0 m. These results do not align with corresponding observations, which range from −13.01 – 4.59 m (mean = −0.01 m) in NY, −11.26 – 16.23 m (mean = 5.03 m) in PR, and −11.64 – 42.22 m (mean = 15.15 m) in SC (Fig. 8). Also, the longshore trends (accretion and erosion) in these predictions do not converge with those observed, evident by a Spearman's correlation (r_s) of 0.06 ($p = 0.003$) in NY, 0.23 ($p < 0.01$) in PR, and −0.247 ($p < 0.01$) in SC, and a *BSS* = 0 in PR and SC. However, the Bruun Rule micro-timescale predictions and associated observations in NY both indicate net erosion, hence a *BSS* of 0.2. The Bruun Rule's ability to predict the correct net shoreline change trend here is not adequate from a coastal management perspective, as realistic predictions of shoreline change trends *and* magnitudes are needed to inform effective coastal management. Under- and over-predictions of shoreline change magnitudes not only compromise the efficacy of coastal management decisions, but also generate economic (e.g., increased financial cost to redesign schemes), morphological (e.g., sediment starvation arising from poorly placed structures), and hazard (e.g., coastal inundation arising from poorly conceived flood defences) risks (Seenath et al., 2016; Pourkerman et al., 2022). The negligible Bruun Rule predictions here correspond to *SLR* being almost 0 m in each site over the micro timescales considered. As *SLR* provides the only forcing in the Bruun Rule, the total magnitude of *SLR* directly affects the magnitude of its shoreline change predictions.

We see a closer fit between micro-timescale shoreline change observations and predictions from Seenath (2022b)'s MIKE21 models in each site (Fig. 9), evident by *BSS* s = 0.2 (SC), 0.4 (PR), and 0.5 (NY). These *BSS* s correspond to MIKE21 predictions and associated observations both showing: net erosion in NY and net accretion in PR and SC; consistent longshore trends in shoreline change, evident by most transects recording the same trend observed and predicted (65% in NY; 77% in PR; 54% in SC). Also, compared to the Bruun Rule, MIKE21 micro-timescale accretion and erosion predictions longshore better align with those observed in each test site, evident from the mean absolute shoreline change (MAC) statistics in Figs. 8–9.

We acknowledge that a rise in relative sea-level over micro timescales is not realistically expected to result in a detectable change in shoreline position, which explains the Bruun Rule poor performance above. However, we observe an average shoreline change up to ~15 m over the micro-timescale considered in each site (Figs. 8–9), which correspond to variations in nearshore circulation in response to local factors (e.g., storminess, coastal structures) (Gallien et al., 2015; USACE & NYSDEC, 2015; Barreto, 2017). The magnitude and patterns of observed micro-timescale shoreline change in each site is generally replicated by MIKE21 (Fig. 9), which accounts for this variability in

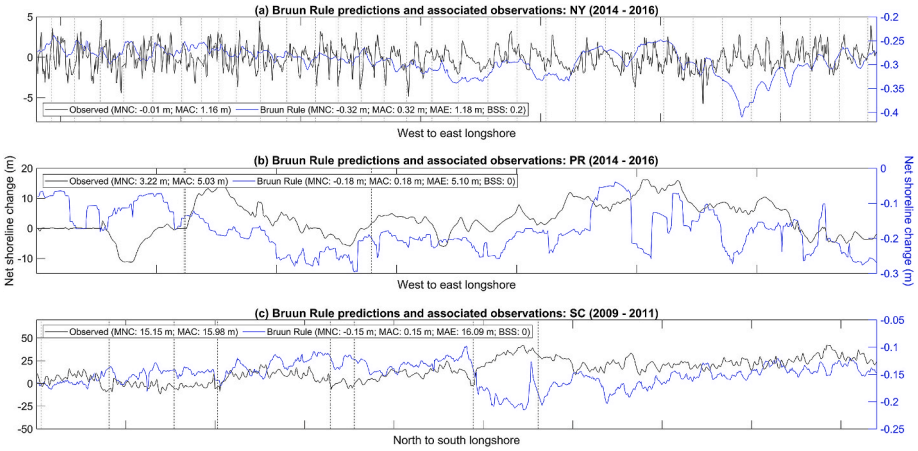

Fig. 8. The Bruun Rule micro-timescale predictions of shoreline change in NY (2014–2016) (a), PR (2014–2016) (b), and SC (2009–2011) (c). Vertical dashed lines = groyne locations. MNC = mean net change, MAC = mean absolute change, MAE = mean absolute error, and BSS = Brier Skill score. Note there is a separate *y* axis for shoreline change observed and predicted from the Bruun Rule in (a) to (c). Shoreline change observed and predicted in groyne transects are excluded from the above data.

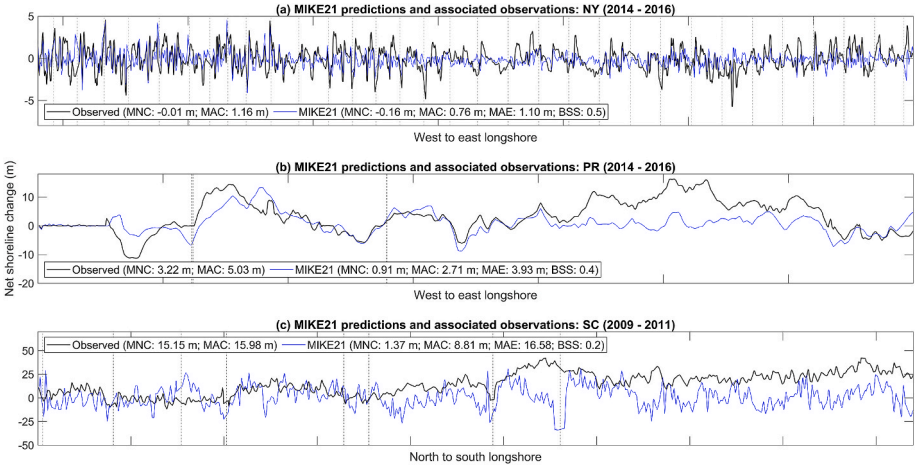

Fig. 9. Seenath (2022b)'s MIKE21 micro-timescale predictions of shoreline change in NY (2014–2016) (a), PR (2014–2016) (b), and SC (2009–2011) (c). Shoreline change observed and predicted in groyne transects are excluded from the above data.

nearshore circulation. The cumulative effects of local drivers operating over the micro-timescale, such as storms, can influence the patterns of shoreline change we see over meso-timescales (Kombiadou et al., 2019; Anthony and Aagaard, 2020; Toimil et al., 2020).

In some cases, meso-timescale shoreline change rates resulting from the cumulative effect of micro-timescale variations in local drivers can be greater than the baseline meso-timescale shoreline change rate expected from *SLR* alone (Slott et al., 2006). Therefore, while we cannot expect the Bruun Rule to predict realistic micro-timescale shoreline change (as it accounts for *SLR* only), applying the rule over micro and longer timescales and comparing the results with observations and predictions from models that account for nearshore circulation (as we have done) can enable us to assess the relative effects of combined local factors and *SLR* on shoreline change across timescales. Such knowledge is crucial for developing more robust shoreline models to better support coastal management, especially given the assumption in related studies that *SLR* is the main driver of shoreline change (e.g., Ritphring et al., 2018; Udo and Takeda, 2018; Sharaan and Udo, 2020; Bagheri et al., 2023).

Deconstructing the functional form of both models and considering the above findings, it is evident that nearshore circulation (which underpins MIKE21 sediment transport predictions) has a greater influence on micro-timescale shoreline change than *SLR* induced cross-shore transport (which drives the Bruun Rule). These findings align with those of Slott et al. (2010) and Stive et al. (2002). Nearshore circulation is a collective term used to describe the complex interconnected nearshore currents that arise from wave interactions with local factors within and near the breaker zone (Shepard and Inman, 1950). It consists of shoreward directed currents (rip feeders), longshore currents, and seaward directed currents (undertow and rip). Nearshore circulation affects longshore and cross-shore sediment transport, which act together to evolve the coastal profile and influence shoreline morphology over timescales up to 10^1 years (Stive et al., 2002). MIKE21 accounts for the detailed structure of the nearshore circulation by coupling a 2D wave, flow, and sediment transport model. This enables MIKE21 to simulate sediment transport in response to the combined interactions of coastal processes, local morphology, coastal management, and *SLR* rate (Seenath, 2022b). *SLR*, however, will likely have a greater influence on shoreline change over meso-timescales (Stive et al., 2002). Current theoretical expectations are that the Bruun Rule predictions may be more realistic over such timescales, especially as the natural response of beaches to *SLR* is inland migration (Cooper et al., 2020).

Contrary to theoretical expectations, the Bruun Rule fails to hindcast observed shoreline change in NY from 1966 to 2016, evident by a $BSS = -13$, corresponding to the rule predicting erosion longshore instead of the net accretion observed under the 0.2 m *SLR* over this period (NOAA,

2017d) (Fig. 10). The Bruun Rule assumes linearity between *SLR* and shoreline change and will, therefore, always predict erosion in response to *SLR* (Bruun, 1962; Ranasinghe et al., 2012; Le Cozannet et al., 2016). This linear assumption fails to account for the nearshore circulation influence on sediment dynamics, which, in some cases, may offset the erosion effects of *SLR*, particularly in environments where natural (e.g., reefs) and human (e.g., groynes) shore protection structures counteract wave impacts (Slott et al., 2010; Barreto, 2017; Cooper et al., 2020). The key insights of the Bruun Rule results here are that *SLR* is not always the primary driver of meso-timescale shoreline change as the Rule assumes, and does not necessarily threaten the existence of sandy coastlines as often reported in Bruun Rule studies (e.g., Hinkel et al., 2013; Sharaan and Udo, 2020; Vousdoukas et al., 2020). These insights are further supported by Seenath (2022a)'s MIKE21 hindcast predictions of shoreline change from 1966 to 2016 in NY having a higher accuracy (*BSS* = 0.2) than that of the Bruun Rule (*BSS* = −13), and indicating net accretion in line with observed trends (Fig. 10). Also, shoreline change observations (67% accretion; 33% erosion) and predictions from MIKE21 (60% accretion; 40% erosion) over this 50-year hindcast both converged, indicating accretion dominated ≥60% of the area with higher accretion than erosion magnitudes longshore (Fig. 10).

The net accretion observed from 1966 to 2016 in NY is mainly attributed to groynes constructed between 1930 and 1961, and secondarily attributed to periodic beach feeding on the north east of the island (Tanski, 2012; Catania, 2015; USACE & NYSDEC, 2015). Prior to the groynes, the shoreline was retreating (Gornitz et al., 2002; Tanski, 2012). The groynes here are effective at trapping sediment discharged from the Jones Inlet (east coast of NY), which then travels west along the Atlantic coast of NY via longshore currents.

In addition to more accurate predictions, MIKE21 predicts the alternating pattern of accretion and erosion observed from 1966 to 2016 in NY, with accretion mainly between groynes and erosion mostly in the immediate vicinity of groynes (Fig. 10). This alternating pattern is common in groyne fields, such as in NY (Fig. 2), that intercept longshore sediment transport to facilitate shoreline stabilisation and expansion of beach width (Hapke et al., 2013; Ruiz-Martínez et al., 2016). MIKE21's ability to produce more accurate meso-timescale predictions (*BSS* = 0.2) compared to the Bruun Rule (*BSS* = −13) in NY provides empirical evidence of the importance of accounting for nearshore circulation in shoreline models. The wider implication of these results is that shoreline response to *SLR* over meso-timescales depends on a number of local factors and processes and not just the total amount of *SLR* as the Bruun Rule assumes, which is consistent with the arguments of Cooper and Pilkey (2004) and Cooper et al. (2020).

MIKE21's ability to replicate observed trends over the micro and meso-timescale hindcasts gives us the confidence to use its meso-timescale projections as a benchmark for evaluating the suitability of applying the Bruun Rule to project future shoreline change. Considering historical meso-timescale shoreline change trends in NY (1966–2016) and PR (1936–2017), we obtain more realistic projections of future shoreline response (2014–2064) to a 0.28 m *SLR* from MIKE21 than the Bruun Rule in both sites (Fig. 11).

In NY, MIKE21 projects: an alternating pattern of accretion and erosion longshore, with accretion mainly between groynes and erosion mainly in the direct vicinity of groynes, in line with realistic expectations (Fig. 10; 11a); net accretion (mean net change = 1.02 m; standard deviation = 5.68) consistent with meso-timescale trends observed under past *SLR* (Fig. 10; 11a); higher erosion magnitudes (mean = 4.03 m) than observed from 1966 to 2016 (mean = 3.08 m) as expected from a higher rise in *SLR* (Fig. 10; 11a). For context here, *SLR* from 1966 to 2016 in NY was 0.2 m whereas we use a 0.28 m *SLR* to project shoreline change from 2014 to 2064. As expected, the Bruun Rule only predicts erosion longshore as a consequence of its inability to account for the groynes in NY by assuming linearity between *SLR* and shoreline change.

We acknowledge that the Bruun Rule is designed to give an initial assessment of the impact of *SLR* alone (and not that of groynes) on shoreline change (Bruun, 1983, 1988), however the magnitude of shoreline change from *SLR* alone is likely to differ significantly from the magnitude of shoreline change expected from combined natural and human forcings. This is evident from our results here and those of Slott et al. (2006). Yet, the Bruun Rule is extensively applied to inform the management of natural and managed sandy coasts across local, regional and global scales (Baron et al., 2014; Carrasco et al., 2016; Walker et al., 2017; Udo and Takeda, 2018; Athanasiou et al., 2019; Vousdoukas et al., 2020; Harley et al., 2022) for two reasons: (a) easy application; (b) popular belief that *SLR* 'threatens' the existence of sandy beaches, amplifying the urgency of projecting shoreline change in response to *SLR*, which it facilitates.

Specifically, our NY results demonstrate that the Bruun Rule provides a misleading assessment of shoreline change since *SLR* does not affect the coast in isolation. Instead, it interacts with local factors (natural and human), and it is this interaction which significantly influences coastal morphology. We, therefore, need to carefully consider this when applying the Bruun Rule to inform the management of sandy coastal systems, particularly since most of these systems are now extensively occupied by humans and managed by some form of engineering (Schlacher et al., 2008; Nurse et al., 2014; Luijendijk et al., 2018; Jackson and Nordstrom, 2020).

In PR, MIKE21 projects net accretion (mean net change = 4.6 m; standard deviation = 21.78), with accretion dominating 59% of the site,

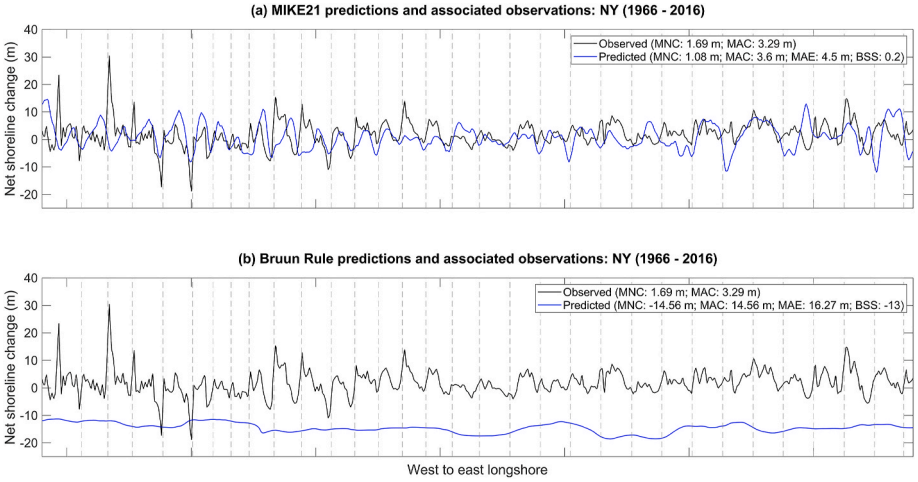

Fig. 10. 1966–2016 predictions of shoreline change in NY from Seenath (2022a)'s MIKE21 meso-timescale model for this site (a) and the Bruun Rule (b). Shoreline change observed and predicted in groyne transects are excluded from the above plots and statistics.

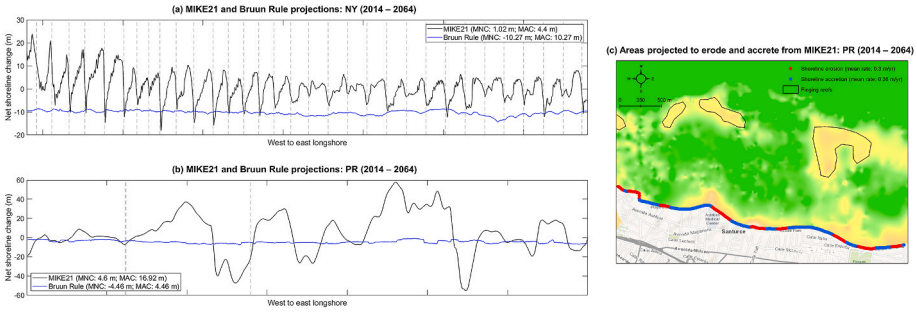

Fig. 11. 2014–2064 MIKE21 and the Bruun Rule shoreline change projections for NY (a) and PR (b). (c) Shows the longshore accretion and erosion trends projected from MIKE21 in PR. Shoreline change projected in groyne transects are excluded from the above plots and statistics.

and higher accretion magnitudes (mean = 18.16 m) than erosion magnitudes (mean = 15.12 m) longshore (Fig. 11b). These predictions are consistent with historical meso-timescale shoreline change trends at the site. From 1936 to 2017, the shoreline in PR accreted along areas buffered by reefs and mangroves at rates of 0.3–0.5 m yr^{-1} and eroded in areas with no natural protection at rates of 0.2–1.21 m yr^{-1} (Barreto, 1997, 2017; Morelock and Barreto-Orta, 2003; Barreto-Orta et al., 2019). These historical trends are generally replicated by MIKE21 (Fig. 11c), which predicts a mean accretion rate of 0.36 m yr^{-1} in reef areas and a mean erosion rate of 0.3 m yr^{-1} in non-reef areas from 2014 to 2064. It is worth noting that the reefs in PR are discretised in the mesh used to apply MIKE21 here (Fig. 12). MIKE21, therefore, inherently accounted for their dissipative impacts on wave action and ensuing nearshore currents in sediment transport simulations (Fig. 12). The 1936 to 2017 shoreline trends in PR indicate that the reefs and mangroves at the site facilitated net accretion over an 81-year period of *SLR*. The exact amount of *SLR* over this period in PR is unknown. However, PR had an overall *SLR* of 0.11 m from 1962 to 2017 (NOAA, 2017c). MIKE21's ability to predict net accretion in response to reefs under a 0.28 m *SLR* in PR is, therefore, in line with *theoretically realistic* expectations relative to the associated Bruun Rule predictions. The Bruun Rule projects erosion longshore (range = −7.39 to −0.97 m; mean net change = −4.46 m; standard deviation = 1.5) (Fig. 11b) as it is unable to account for the reefs natural defence (Goenaga and Cintron, 1979; Barreto-Orta et al., 2019), again due to its assumption of linearity between *SLR* and shoreline change. This assumption implicitly implies that there is always sediment deficit from *SLR*, which is proven otherwise from the historical shoreline change trends in NY and PR.

The functional form of MIKE21 and the Bruun Rule are based on the principles of the equilibrium beach profile theory. Both models assume the active coastal profile shifts shore-normal in response to a change in sediment balance. The key difference is that the movement of the active coastal profile is driven by littoral drift in response to nearshore circulation in MIKE21 and total *SLR* in the Bruun Rule. Despite a notably similar computational structure, our results show that MIKE21 performs considerably better than the Bruun Rule over micro and meso-timescales. Acknowledging this, the assumption of an equilibrium coastal profile appears to be a valid concept for simulating meso-timescale shoreline change. However, the processes that force coastal profiles towards equilibrium in shoreline models need to be carefully considered. In particular, our results indicate that nearshore circulation (which drives MIKE21) in response to the combined effects of local factors (natural and human) has a more significant impact on shoreline change than the magnitude and rate of *SLR* alone (which drives the Bruun Rule).

3.1. *Key governance insights for coastal management*

Our findings reveal three key insights for coastal management. *First*, coastal managers should prioritise understanding the primary drivers of

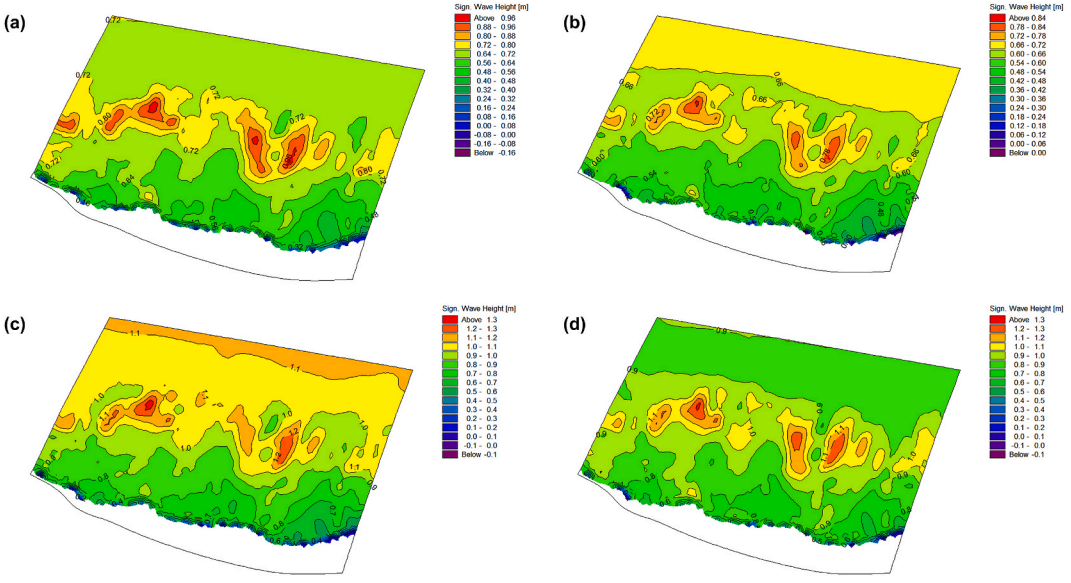

Fig. 12. Significant wave heights generated at different timesteps in MIKE21 meso-timescale shoreline simulation (10-Oct-2014 to 10-Oct-2064) in PR: 10-Oct-2015 00:00:00 (a), 10-Oct-2024 00:00:00 (b), 10-Oct-2034 00:00:00 (c), and 10-Oct-2054 00:00:00 (d). The key take-home message here is that the highest significant wave heights occur near the reefs.

shoreline change when selecting models to simulate and predict shoreline evolution. Using theoretically and physically unrealistic models can undermine the efficacy of management efforts. *Second*, while the Bruun Rule helps establish a baseline shoreline change rate in response to *SLR*, this rate is often significantly smaller than the rate of shoreline change caused by local drivers, such as nearshore circulation. Relying solely on the Bruun Rule may overlook crucial local dynamics, with credibility implications for ensuing coastal management decisions. *Third*, hybrid shoreline models, like MIKE21, are effective for the timescales relevant to coastal management but require extensive datasets, which limit the practical application of these models in resource-poor areas, characteristic of vulnerable sandy coasts in small islands where shoreline models are needed as coastal management tools. We, therefore, need to focus more on identifying an optimal shoreline modelling approach that balances realistic process simulations with manageable data requirements to facilitate practical applications in diverse coastal settings for coastal management decision-making.

4. Conclusions

We provide a unique assessment of the Bruun Rule's suitability for modelling micro and meso-timescale shoreline change in three morphological different sandy coasts by comparing its predictions against: associated observations, verified predictions representative of coastal sediment transport, and historical shoreline change trends observed under past *SLR*. Our results show that the Bruun Rule fails to provide realistic meso-timescale shoreline change predictions in sandy coasts, including those that conform to its morphology assumptions (e.g., NY and SC), primarily because it assumes linearity between *SLR* and shoreline retreat. This restrictive assumption does not allow the Bruun Rule to consider the nearshore circulation, which appears to have a much greater impact on micro and meso-timescale shoreline change than the magnitude and rate of *SLR* alone in sandy coasts. This inference stems from MIKE21 (driven by nearshore circulation) better replicating observed micro and meso-timescale shoreline change in each site than the Bruun Rule (driven by *SLR*).

A particularly interesting and novel aspect of our work is our comparison of the Bruun Rule against a simple one-line shoreline model that is coupled into a complex hybrid model, MIKE21. Given the structure of MIKE21 – which links a coupled 2D wave, flow and sediment transport model with a one-line shoreline model – it can easily be overlooked that such a 'complex' hybrid model essentially equates to a simple rule-based equation like the Bruun Rule for the shoreline morphology update. The complexity of MIKE21 is contained to the sediment transport predictions, which is an input for the one-line equation embedded into its computational structure similar to *SLR* (which, in this study, is derived from long-term tidal records representative of local water level variations) being an input into the Bruun Rule equation. What we have shown is that the equilibrium beach profile modelling approach – which underpins the shoreline morphology update in both models – is valid for modelling micro and meso-timescale shoreline change in sandy coasts, evident from the plausible results obtained from MIKE21. However, we show that the validity of such an approach for modelling shoreline change depends on the internal forcing used to update the shoreline morphology. Specifically, we show that, for such an approach to produce theoretically and physically realistic results, the internal forcing used to drive shoreline change needs to be representative of the underlying physics of coastal sediment transport. Our results suggest that equilibrium beach profile models driven by nearshore circulation are more suitable for modelling shoreline change in sandy coasts than related models driven by rates and magnitudes of *SLR* alone. Considering how important shoreline models are for informing adaptive responses to coastal change alongside our findings, we, therefore, recommend limiting the use of the Bruun Rule for informing policy and the management of sandy coasts.

CRediT authorship contribution statement

Avidesh Seenath: Writing – review & editing, Writing – original draft, Visualization, Validation, Methodology, Formal analysis, Data curation, Conceptualization. **Jonathan Dale:** Writing – review & editing, Writing – original draft, Conceptualization.

Declaration of competing interest

The authors declare that they have no known competing financial interests or personal relationships that could have appeared to influence the work reported in this paper.

Data availability

Data will be made available on request.

Acknowledgements

The modelling work in this paper originates from a PhD thesis undertaken by Avidesh Seenath at Durham University. Many thanks to the PhD advisory committee, DHI Water Environments UK Ltd for giving access to MIKE21, and Mark Bailes for his support with the software. We are also grateful to the participants of the 2023 Coastal Zone Canada Conference for providing constructive feedback that helped to improve the quality and clarity of the paper.

References

Almeida, L.P., Efraim De Oliveira, I., Lyra, R., Scaranto Dazzi, R.L., Martins, V.G., Henrique Da Fontoura Klein, A., 2021. Coastal analyst system from space imagery engine (Cassie): shoreline management module. Environ. Model. Software 140.
Álvarez-Cuesta, M., Losada, I.J., Toimil, A., 2023. A nearshore evolution model for sandy coasts: IH-LANSloc. Environ. Model. Software 169.
Anthony, E.J., Aagaard, T., 2020. The lower shoreface: morphodynamics and sediment connectivity with the upper shoreface and beach. Earth Sci. Rev. 210.
Ashton, A.D., Murray, A.B., 2006. High-angle wave instability and emergent shoreline shapes: 1. Modeling of sand waves, flying spits, and capes. J. Geophys. Res.: Earth Surf. 111, F04011.
Athanasiou, P., Van Dongeren, A., Giardino, A., Vousdoukas, M., Gaytan-Aguilar, S., Ranasinghe, R., 2019. Global distribution of nearshore slopes with implications for coastal retreat. Earth Syst. Sci. Data 11, 1515–1529.
Athanasiou, P., Van Dongeren, A., Giardino, A., Vousdoukas, M.I., Ranasinghe, R., Kwadijk, J., 2020. Uncertainties in projections of sandy beach erosion due to sea level rise: an analysis at the European scale. Sci. Rep. 10, 11895.
Bagheri, M., Ibrahim, Z.Z., Mansor, S., Manaf, L.A., Akhir, M.F., Talaat, W.I.a.W., Wolf, I.D., 2023. Hazard assessment and modeling of erosion and sea level rise under global climate change conditions for coastal city management. Nat. Hazards Rev. 24, 04022038.
Barkwith, A., Thomas, C.W., Limber, P.W., Ellis, M.A., Murray, A.B., 2014. Coastal vulnerability of a pinned, soft-cliff coastline Part I: assessing the natural sensitivity to wave climate. Earth Surf. Dyn. 2, 295–308.
Baron, H.M., Ruggiero, P., Wood, N.J., Harris, E.L., Allan, J., Komar, P.D., Corcoran, P., 2014. Incorporating climate change and morphological uncertainty into coastal change hazard assessments. Nat. Hazards 75, 2081–2102.
Barreto-Orta, M., Mendez-Tejeda, R., Rodriguez, E., Cabrera, N., Diaz, E., Perez, K., 2019. State of the beaches in Puerto Rico after hurricane Maria (2017). Shore Beach 87, 16–23.
Barreto, M., 1997. Shoreline changes in Puerto Rico (1936-1993). Doctor of Philosophy in Marine Sciences. University of Puerto Rico.
Barreto, M., 2017. Assessment of Beach Morphology at Puerto Rico Island. University of Puerto Rico, Puerto Rico.
Bruun, P., 1954. *Coast Erosion and the Development of Beach Profiles*, U.S. Beach Erosion Board.
Bruun, P., 1962. Sea-level rise as a cause of shore erosion. J. Waterw. Harb. Div. 88, 117–130.
Bruun, P., 1983. Review of conditions for uses of the Bruun rule of erosion. Coast Eng. 7, 77–89.
Bruun, P., 1988. The Bruun rule of erosion by sea-level rise: a discussion on large-scale two- and three-dimensional usages. J. Coast Res. 4, 627–648.
Burningham, H., French, J., 2017. Understanding coastal change using shoreline trend analysis supported by cluster-based segmentation. Geomorphology 282, 131–149.
Carrasco, A.R., Ferreira, Ó., Roelvink, D., 2016. Coastal lagoons and rising sea level: a review. Earth Sci. Rev. 154, 356–368.
Catania, J.A., 2015. Analysis of Infrastructure Damage after Superstorm Sandy: A Case Study of Long Beach. East Carolina University, NY.

Cooper, J.a.G., Green, A.N., Loureiro, C., 2018. Geological constraints on mesoscale coastal barrier behaviour. Global Planet. Change 168, 15–34.
Cooper, J.a.G., Masselink, G., Coco, G., Short, A.D., Castelle, B., Rogers, B., Anthony, E., Green, A.N., Kelley, J.T., Pilkey, O.H., Jackson, D.W.T., 2020. Sandy beaches can survive sea-level rise. Nat. Clim. Change 10, 993–995.
Cooper, J.a.G., Pilkey, O.H., 2004. Sea-level rise and shoreline retreat: time to abandon the Bruun rule. Global Planet. Change 43, 157–171.
Cowell, P.J., Kench, P.S., 2001. The morphological response of atoll islands to seasea-level rise. Part 1: modifications to the shoreface translation model. J. Coast Res. 633–644. www.jstor.org/stable/25736329.
Cowell, P.J., Roy, P.S., Jones, R.A., 1992. Shoreface translation model: computer simulation of coastal-sand-body response to sea level rise. Math. Comput. Simulat. 33, 603–608.
Cutler, E.M., Albert, M.R., White, K.D., 2020. Tradeoffs between beach nourishment and managed retreat: insights from dynamic programming for climate adaptation decisions. Environ. Model. Software 125.
Dastgheib, A., Martinez, C., Udo, K., Ranasinghe, R., 2022. Climate change driven shoreline change at hasaki beach Japan: a novel application of the probabilistic coastline recession (PCR) model. Coast Eng. 172.
DHI, 2017. MIKE 21 documentation [Online]. Available: https://manuals.mikepowerdbydhi.help/2017/MIKE_21.htm. (Accessed 1 January 2017).
Eversole, D., Fletcher, C.H., 2003. Longshore sediment transport rates on a reef-fronted beach: field data and empirical models kaanapali beach, Hawaii. J. Coast Res. 19, 649–663.
Gallien, T.W., O'reilly, W.C., Flick, R.E., Guza, R.T., 2015. Geometric properties of anthropogenic flood control berms on southern California beaches. Ocean Coast Manag. 105, 35–47.
Goenaga, C., Cintron, G., 1979. Inventory of the Puerto Rican coral reefs. Puerto Rico Department of Natural Resources.
Gornitz, V., Couch, S., Hartig, E.K., 2002. Impacts of sea level rise in the New York city Metropolitan area. Global Planet. Change 32, 61–68.
Hallin, C., Larson, M., Hanson, H., 2019. Simulating beach and dune evolution at decadal to centennial scale under rising sea levels. PLoS One 14, e0215651.
Hapke, C.J., Kratzmann, M.G., Himmelstoss, E.A., 2013. Geomorphic and human influence on large-scale coastal change. Geomorphology 199, 160–170.
Harley, M.D., Masselink, G., Ruiz De Alegría-Arzaburu, A., Valiente, N.G., Scott, T., 2022. Single extreme storm sequence can offset decades of shoreline retreat projected to result from seasea-level rise. Commun. Earth Environ. 3.
Hinkel, J., Nicholls, R.J., Tol, R.S.J., Wang, Z.B., Hamilton, J.M., Boot, G., Vafeidis, A.T., Mcfadden, L., Ganopolski, A., Klein, R.J.T., 2013. A global analysis of erosion of sandy beaches and sea-level rise: an application of diva. Global Planet. Change 111, 150–158.
Hippensteel, S., 2019. In: Gámez, J.L.S., Lin, Z., Nesbit, J. (Eds.), The Impact of Future Sea-Level Rise on Rio De Janeiro: A Geological Perspective. Routledge. *Rio De Janeiro*.
Hoozemans, F.M.J., Marchand, M., Pennekamp, H.A., 1993. A global vulnerability assessment: vulnerability assessments for population. In: Coastal Wetlands and Rice Production on a Global Scale. , The Netherlands. Delft Hyrdaulics.
Itzkin, M., Moore, L.J., Ruggiero, P., Hovenga, P.A., Hacker, S.D., 2022. Combining process-based and data-driven approaches to forecast beach and dune change. Environ. Model. Software 153.
Jackson, N.L., Nordstrom, K.F., 2020. Trends in research on beaches and dunes on sandy shores, 1969–2019. Geomorphology 366, 106737.
Kaergaard, K., Fredsoe, J., 2013. A numerical shoreline model for shorelines with large curvature. Coast Eng. 74, 19–32.
Karunarathna, H., Horrillo-Caraballo, J., Kuriyama, Y., Mase, H., Ranasinghe, R., Reeve, D.E., 2016. Linkages between sediment composition, wave climate and beach profile variability at multiple timescales. Mar. Geol. 381, 194–208.
Kinsela, M.A., Hanslow, D.J., Carvalho, R.C., Linklater, M., Ingleton, T.C., Morris, B.D., Allen, K.M., Sutherland, M.D., Woodroffe, C.D., 2020. Mapping the shoreface of coastal sediment compartments to improve shoreline change forecasts in new South wales, Australia. Estuar. Coast. https://doi.org/10.1007/s12237-020-00756-7.
Kombiadou, K., Costas, S., Carrasco, A.R., Plomaritis, T.A., Ferreira, Ó., Matias, A., 2019. Bridging the gap between resilience and geomorphology of complex coastal systems. Earth Sci. Rev. 198.
Le Cozannet, G., Bulteau, T., Castelle, B., Ranasinghe, R., Woppelmann, G., Rohmer, J., Bernon, N., Idier, D., Louisor, J., Salas, Y.M.D., 2019. Quantifying uncertainties of sandy shoreline change projections as sea level rises. Sci. Rep. 9, 42.
Le Cozannet, G., Garcin, M., Yates, M., Idier, D., Meyssignac, B., 2014. Approaches to evaluate the recent impacts of sea-level rise on shoreline changes. Earth Sci. Rev. 138, 47–60.
Le Cozannet, G., Oliveros, C., Castelle, B., Garcin, M., Idier, D., Pedreros, R., Rohmer, J., 2016. Uncertainties in sandy shorelines evolution under the Bruun rule assumption. Front. Mar. Sci. 3, 49.
Luijendijk, A., Hagenaars, G., Ranasinghe, R., Baart, F., Donchyts, G., Aarninkhof, S., 2018. The state of the world's beaches. Sci. Rep. 8, 6641.
Malcolm, J.B., Janet, M.H., 1997. Prediction of soft-cliff retreat with accelerating sea-level rise. J. Coast Res. 13, 453–467.
Masselink, G., Brooks, S., Poate, T., Stokes, C., Scott, T., 2022. Coastal dune dynamics in embayed settings with sea-level rise – examples from the exposed and macrotidal north coast of Sw England. Mar. Geol. 450.
McLean, R.F., 2013. Bruun rule. In: Goudie, A. (Ed.), Encyclopedia of Geomorphology. Taylor & Francis.
Meyer, M., Harff, J., Gogina, M., Barthel, A., 2008. Coastline changes of the Darss–Zingst Peninsula — a modelling approach. J. Mar. Syst. 74, S147–S154.
Morelock, J., Barreto-Orta, M., 2003. An update of coastal erosion in Puerto Rico. Shore Beach 71, 7–12.
Mueller, N.J., Meindl, C.F., 2017. Vulnerability of Caribbean island cemeteries to sea level rise and storm surge. Coast. Manag. 45, 277–292.
Mycoo, M., Donovan, M.G., 2017. A blue urban Agenda: adapting to climate change in the coastal cities of Caribbean. Pacific Small Island Developing States. Inter-American Development Bank.
NCEI, 2017a. NCEI hurricane sandy digital elevation models [Online]. Available: https://www.ngdc.noaa.gov/mgg/inundation/sandy/sandy_geoc.html. (Accessed 3 March 2017).
NCEI, 2017b. Santa Monica, California 1/3 Arc-second NAVD 88 coastal digital elevation model [Online]. Available: https://data.noaa.gov//metaview/page?xml=NOAA/NESDIS/NGDC/MGG/DEM/iso/xml/726.xml&view=getDataView&header=none. (Accessed 3 March 2017).
NCEI, 2019. San juan, Puerto Rico 1/9 arc-second PRVD coastal digital elevation model [Online]. Available: https://www.ncei.noaa.gov/metadata/geoportal/rest/metadata/item/gov.noaa.ngdc.mgg.dem:11510/html. (Accessed 1 June 2019).
NDBC, 2017a. NDBC- station 44065 recent data [Online]. Available: https://www.ndbc.noaa.gov/station_page.php?station=44065. (Accessed 1 January 2017).
NDBC, 2017b. NDBC - station 41053 recent data [Online]. Available: https://www.ndbc.noaa.gov/station_page.php?station=41053. (Accessed 1 January 2017).
NDBC, 2017c. NDBC - station 46221 recent data [Online]. Available: https://www.ndbc.noaa.gov/station_page.php?station=46221. (Accessed 3 March 2017).
Nguyen, Q.H., Takewaka, S., 2020. Land subsidence and its effects on coastal erosion in the Nam Dinh coast (Vietnam). Continent. Shelf Res. 207.
Nicholls, R.J., Birkemeier, W.A., Hallermeier, R.J., 1996. Application of the depth of closure concept. In: 25th International Conference on Coastal Engineering, 1996 Florida, USA, pp. 3874–3887.
Nicholls, R.J., Cazenave, A., 2010. Sea-level rise and its impact on coastal zones. Science 328, 1517–1520.
NOAA, 2017a. 2009 - 2011 CA coastal conservancy coastal lidar project: hydro-flattened bare Earth DEM [Online]. Available: https://coast.noaa.gov/htdata/raster2/elevation/California_Lidar_DEM_2009_1131/ca2010_coastal_dem.html. (Accessed 3 March 2017).
NOAA, 2017b. 2016 USGS CoNED topobathymetric model (1887 - 2016). New England [Online]. Available: https://inport.nmfs.noaa.gov/inport/item/49419/citation. (Accessed 3 March 2017).
NOAA, 2017c. San Juan, La Puntilla. San Juan Bay. *Pr - Station Id: 9755371* [Online]. Available: https://tidesandcurrents.noaa.gov/stationhome.html?id=9755371. (Accessed 1 January 2017).
NOAA, 2017d. Sandy hook, NJ - station id: 8531680 [Online]. Available: https://tidesandcurrents.noaa.gov/stationhome.html?id=8531680. (Accessed 17 November 2017).
NOAA, 2017e. *Santa Monica, CA - Station Id: 9410840* [Online]. Available: https://tidesandcurrents.noaa.gov/stationhome.html?id=9410840. (Accessed 3 March 2017).
NOAA, 2019. 2016 NOAA NGS topobathy Lidar DEM: Puerto Rico [Online]. Available: https://coast.noaa.gov/htdata/raster2/elevation/NGS_PR_DEM_2016_8462/. (Accessed 1 June 2019).
Nurse, L.A., McLean, R.F., Agard, J., Briguglio, L.P., Duvat-Magnan, V., Pelesikoti, N., Tompkins, E., Webb, A., 2014. Small islands. In: Barros, V.R., Field, C.B., Dokken, D.J., Mastrandrea, M.D., Mach, K.J., Bilir, T.E., Chatterjee, M., Ebi, K.L., Estrada, Y.O., Genova, R.C., Girma, B., Kissel, E.S., Levy, A.N., Maccracken, S., Mastrandrea, P.R., White, L.L. (Eds.), Climate Change 2014: Impacts, Adaptation, and Vulnerability. Part B: Regional Aspects. Contribution of Working Group Ii to the Fifth Assessment Report of the Intergovernmental Panel of Climate Change. Cambridge University Press, Cambridge, United Kingdom and New York, NY, USA.
Paneque, R.R., Finkl, C.W., 2020. Erosion of Carbonate beaches on the Northeastern coast of Cuba. J. Coast Res. 36.
Pathak, A., Van Beynen, P.E., Akiwumi, F.A., Lindeman, K.C., 2021. Impacts of climate change on the Tourism sector of a small island developing state: a case study for the Bahamas. Environ Dev 37, 100556.
Pontee, N.I., Pye, K., Blott, S.J., 2004. Morphodynamic behaviour and sedimentary variation of mixed sand and gravel beaches, suffolk, UK. J. Coast Res. 20, 256–276.
Pörtner, H.-O., Roberts, D.C., Masson-Delmotte, V., Zhai, P., Tignor, M., Poloczanska, E., Mintenbeck, K., Nicolai, M., Okem, A., Petzold, J., 2019. Ipcc Special Report on the Ocean and Cryosphere in a Changing Climate. Intergovernmental Panel on Climate Change, Geneva, Switzerland.
Pourkerman, M., Marriner, N., Hamzeh, M.-A., Lahijani, H., Morhange, C., Amjadi, S., Vacchi, M., Maghsoudi, M., Shah-Hosseini, M., Afarin, M., 2022. Socioeconomic impacts of environmental risks in the western makran zone (Chabahar, Iran). Nat. Hazards 112, 1823–1849.
Ranasinghe, R., 2020. On the need for a new generation of coastal change models for the 21(St) century. Sci. Rep. 10, 2010.
Ranasinghe, R., Callaghan, D., Stive, M.J.F., 2012. Estimating coastal recession due to sea level rise: beyond the Bruun rule. Climatic Change 110, 561–574.
Ritphring, S., Somphong, C., Udo, K., Kazama, S., 2018. Projections of future beach loss due to sea level rise for sandy beaches along Thailand's coastlines. J. Coast Res. 85, 541–545.
Robinet, A., Idier, D., Castelle, B., Marieu, V., 2018. A reduced-complexity shoreline change model combining longshore and cross-shore processes: the lx-shore model. Environ. Model. Software 109, 1–16.
Ruiz-Martínez, G., Mariño-Tapia, I., Baldwin, E.G.M., Casarín, R.S., Ortiz, C.E.E., 2016. Identifying coastal defence schemes through morphodynamic numerical simulations along the northern coast of yucatan, Mexico. J. Coast Res. 32, 651–669.

Schlacher, T.A., Schoeman, D.S., Dugan, J., Lastra, M., Jones, A., Scapini, F., Mclachlan, A., 2008. Sandy beach ecosystems: key features, sampling issues, management challenges and climate change impacts. Mar. Ecol. 29, 70–90.
Seenath, A., 2022a. A new approach for incorporating sea-level rise in hybrid 2D/one-line shoreline models. Sci. Rep. 12, 18074.
Seenath, A., 2022b. On simulating shoreline evolution using a hybrid 2D/one-line model. Coast Eng. 178, 104216.
Seenath, A., 2023. A new approach for handling complex morphologies in hybrid shoreline evolution models. Appl. Ocean Res. 141.
Seenath, A., Wilson, M., Miller, K., 2016. Hydrodynamic versus gis modelling for coastal flood vulnerability assessment: which is better for guiding coastal management? Ocean Coast Manag. 120, 99–109.
Sharaan, M., Udo, K., 2020. Projections of future beach loss along the mediterranean coastline of Egypt due to seasea-level rise. Appl. Ocean Res. 94, 101972.
Shepard, F.P., Inman, D.L., 1950. Nearshore circulation. Coastal Eng. Proc. 1.
Slott, J.M., Murray, A.B., Ashton, A.D., 2010. Large-scale responses of complex-shaped coastlines to local shoreline stabilization and climate change. J. Geophys. Res.: Earth Surf. 115, F03033.
Slott, J.M., Murray, A.B., Ashton, A.D., Crowley, T.J., 2006. Coastline responses to changing storm patterns. Geophys. Res. Lett. 33, L18404.
Stive, M.J.F., Aarninkhof, S.G.J., Hamm, L., Hanson, H., Larson, M., Wijnberg, K.M., Nicholls, R.J., Capobianco, M., 2002. Variability of shore and shoreline evolution. Coast Eng. 47, 211–235.
Stripling, S., Panzeri, M., Blanco, B., Rossington, K., Sayers, P., Borthwick, A., 2017. Regional-scale probabilistic shoreline evolution modelling for flood-risk assessment. Coast Eng. 121, 129–144.
Sutherland, J., Peet, A.H., Soulsby, R.L., 2004. Evaluating the performance of morphological models. Coast Eng. 51, 917–939.
Tanski, J., 2012. Long Island's Dynamic South Shore - a Primer on the Forces and Trends Shaping Our Coast. New York, USA, New York Sea Grant.
Thiéblemont, R., Le Cozannet, G., Rohmer, J., Toimil, A., Álvarez-Cuesta, M., Losada, I. J., 2021. Deep uncertainties in shoreline change projections: an extra-probabilistic approach applied to sandy beaches. Nat. Hazards Earth Syst. Sci. 21, 2257–2276.
Thiéblemont, R., Le Cozannet, G., Toimil, A., Meyssignac, B., Losada, I.J., 2019. Likely and high-end impacts of regional sea-level rise on the shoreline change of European sandy coasts under a high greenhouse gas emissions scenario. Water 11.
Tinh, N.X., Tanaka, H., Larson, M., 2021. Analytical solution for time-dependent shoreline position response to the tectonic recovery process in the sendai plain, Japan, after the 2011 great east Japan earthquake. Continent. Shelf Res. 231.
Toimil, A., Camus, P., Losada, I.J., Le Cozannet, G., Nicholls, R.J., Idier, D., Maspataud, A., 2020. Climate change-driven coastal erosion modelling in temperate sandy beaches: methods and uncertainty treatment. Earth Sci. Rev. 202.
Udo, K., Takeda, Y., 2018. Projections of future beach loss in Japan due to seasea-level rise and uncertainties in projected beach loss. Coast Eng. J. 59, 1740006-1-1740006-16.
USACE, 2003. Broward County, Shore Protection Project, Segment II and III Renourishment, General Reevaluation Report. Environ. Impact Statement.
USACE & NYSDEC, 2015. Atlantic Coast of Long Island, Jones Inlet to East Rockaway Inlet, Long Beach Island, New York Coastal Storm Risk Management Project: Hurricane Sandy Limited Reevaluation Report Volume 1. Long Beach, NY.
USGS, 2017. Historical topographic maps - preserving the past [Online]. Available: https://www.usgs.gov/programs/national-geospatial-program/topographic-maps. (Accessed 1 January 2017).
Van Maanen, B., Nicholls, R.J., French, J.R., Barkwith, A., Bonaldo, D., Burningham, H., Brad Murray, A., Payo, A., Sutherland, J., Thornhill, G., Townend, I.H., Van Der Wegen, M., Walkden, M.J.A., 2016. Simulating mesoscale coastal evolution for decadal coastal management: a new framework integrating multiple, complementary modelling approaches. Geomorphology 256, 68–80.
Vousdoukas, M.I., Athanasiou, P., Giardino, A., Mentaschi, L., Stocchino, A., Kopp, R.E., Menéndez, P., Beck, M.W., Ranasinghe, R., Feyen, L., 2023. Small island developing States under threat by rising seas even in a 1.5 °C warming World. Nat. Sustain. https://doi.org/10.1038/s41893-023-01230-5.
Vousdoukas, M.I., Ranasinghe, R., Mentaschi, L., Plomaritis, T.A., Athanasiou, P., Luijendijk, A., Feyen, L., 2020. Sandy coastlines under Threat of erosion. Nat. Clim. Change 10, 260–263.
Walker, I.J., Davidson-Arnott, R.G.D., Bauer, B.O., Hesp, P.A., Delgado-Fernandez, I., Ollerhead, J., Smyth, T.a.G., 2017. Scale-dependent perspectives on the geomorphology and evolution of beach-dune systems. Earth Sci. Rev. 171, 220–253.
Warrick, R.A., 2009. From climpacts to simclim: the development of an integrated model for assessing impacts and adaptation to climate change. In: Knight, C.J., Jaeger, J. (Eds.), Integrated Regional Assessment: Challenges and Case Studies. Cambridge University Press, Cambridge, UK.
Young, A.P., Flick, R.E., O'reilly, W.C., Chadwick, D.B., Crampton, W.C., Helly, J.J., 2014. Estimating cliff retreat in southern California considering sea level rise using a sand balance approach. Mar. Geol. 348, 15–26.